JACS
JOURNAL OF THE AMERICAN CHEMICAL SOCIETY
Article
pubs.acs.org/JACS

Probing the Dipolar Coupling in a Heterospin Endohedral Fullerene–Phthalocyanine Dyad

Shen Zhou,[†,∥] Masanori Yamamoto,[‡,∥] G. Andrew D. Briggs,[†] Hiroshi Imahori,*[,‡,§] and Kyriakos Porfyrakis*[,†]

[†]Department of Materials, University of Oxford, Oxford OX1 3PH, U.K.
[‡]Department of Molecular Engineering, Graduate School of Engineering, Kyoto University, Nishikyo-ku, Kyoto 615-8510, Japan
[§]Institute for Integrated Cell-Material Sciences (WPI-iCeMS), Kyoto University, Nishikyo-ku, Kyoto 615-8510, Japan

Supporting Information

ABSTRACT: Paramagnetic endohedral fullerenes and phthalocyanine (Pc) complexes are promising building blocks for molecular quantum information processing, for which tunable dipolar coupling is required. We have linked these two spin qubit candidates together and characterized the resulting electron paramagnetic resonance properties, including the spin dipolar coupling between the fullerene spin and the copper spin. Having interpreted the distance-dependent coupling strength quantitatively and further discussed the antiferromagnetic aggregation effect of the CuPc moieties, we demonstrate two ways of tuning the dipolar coupling in such dyad systems: changing the spacer group and adjusting the solution concentration.

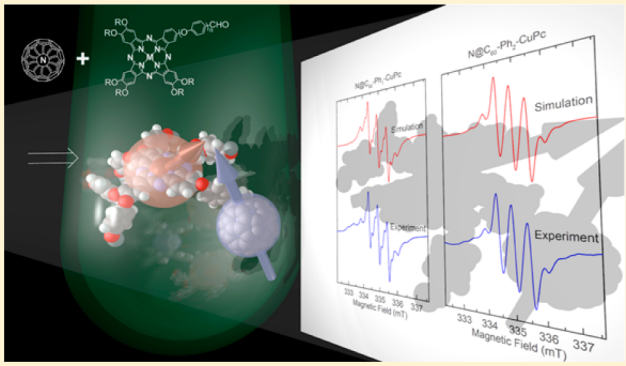

INTRODUCTION

Endohedral fullerenes are molecular carbon cages incarcerating heteroatoms.[1−7] Paramagnetic fullerenes such as N@C_{60}, Sc@C_{82}, Y@C_{82}, and La@C_{82} have relatively long electron spin relaxation times,[8,9] making them candidates for construction of a molecular quantum computer.[10−14] Significant progress has been achieved to date in both theoretical designs, like the proposals of qubit gates,[15−17] and experimental implementations, such as robust phase gates.[18] Realization of a two-qubit gate based on the electron spin with a molecular system remains challenging[19,20] and requires a multispin system with a tunable dipolar coupling effect that could be used to fabricate a two-qubit gate.

Previous studies of multispin endohedral fullerenes have observed electron spin dipolar coupling in the N@C_{60}–CuTPP dyad,[21] FSc_3C_2@C_{80}–PNO$^{\bullet}$,[22] and the N@C_{60}–N@C_{60} dimer.[23] The detailed properties of the dipolar coupling in these endohedral fullerene systems were not fully revealed for various reasons. For the N@C_{60}–CuTPP dyad, the spin signal from the fullerene molecule was completely suppressed by the CuTPP moiety because of the very strong coupling between the spins. In FSc_3C_2@C_{80}–PNO$^{\bullet}$, the complicated hyperfine interaction of the three nonequivalent Sc (I_{Sc} = $^7/_2$) atoms made the spectra difficult to interpret and obscured any effect of dipolar coupling. Studies of dipolar coupling in the N@C_{60}–N@C_{60} dimer have been limited by the purity of N@C_{60}. The broad and weak dipolar coupling signal was masked by the sharp and intense signal originating from the half-filled dimer that was also present.

We have designed and synthesized a series of heterospin systems of endohedral fullerene–phthalocyanine (Pc) dyads. Three main improvements in the molecular design enable us to overcome the limitations listed above: (1) the longer spacer groups between the spin centers avoid the complete suppression phenomenon; (2) we use N@C_{60}, which has a sharper spin signal than Sc_3C_2@C_{80}, as the probing spin to simplify spectral interpretation; and (3) the heterospins resonating at different magnetic fields solve the overlap problem without having to use 100% pure N@C_{60}. Since CuPc has also been suggested as a promising spin qubit candidate,[24,25] the combination of two different spin qubits offers extra possibilities.

We have comprehensively characterized the dipolar coupling effect in the endohedral fullerene–CuPc dyad system for the first time. By comparing the spectral features of dyads having different spin distances, we show that changing the spacer group enables the tuning of the dipolar coupling strength in this system. Utilizing the aggregation and antiferromagnetism of the CuPc moiety, we further demonstrate that the concentration of the sample can also be used to influence the coupling strength in a controllable manner.

RESULTS AND DISCUSSION

Synthesis and Characterization. Three different N@C_{60}–Pc dyads (N@C_{60}-1-CuPc, N@C_{60}-2-CuPc, and N@C_{60}-

Received: November 6, 2015
Published: January 8, 2016

DOI: 10.1021/jacs.5b11641
J. Am. Chem. Soc. 2016, 138, 1313−1319

1-ZnPc) were synthesized by reacting a spin-enriched N@C_{60}/C_{60} mixture (1%) with the corresponding phthalocyanine aldehydes through the 1,3-dipolar cycloadditions shown in Figure 1.[26−28] In order to protect the endohedral fullerene

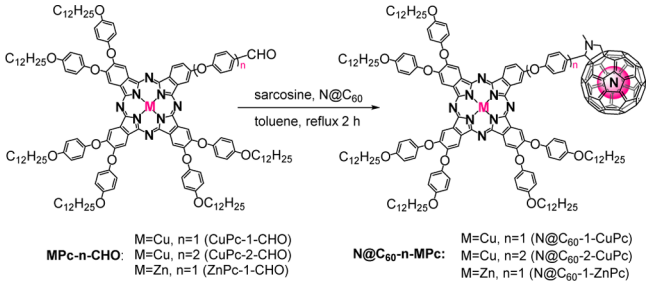

Figure 1. Synthesis of N@C_{60}−phthalocyanine dyads. M represents the copper or zinc ion, and *n* stands for the number of phenoxy groups in the bridging unit.

(derivative), which has limited thermal,[29] irradiative,[30] and chemical stability,[31] we performed the reactions under mild conditions with a compromise on the conversion ratio. The reagents in a stoichiometric ratio dissolved in toluene were refluxed for 2 h in the dark. The product dyads were then isolated from the reaction mixture by high-performance liquid chromatography (HPLC) using a Buckyprep-M column. Figure 2a shows a representative HPLC trace for the separation of N@C_{60}-1-CuPc. Although the yield of the product was relatively low (ca. 22% based on the integrated area percentage of the

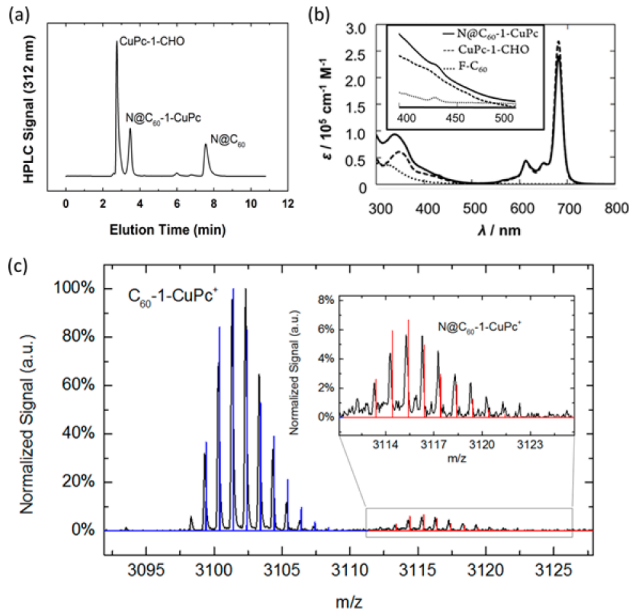

Figure 2. (a) HPLC curve for the separation of N@C_{60}-1-CuPc (Buckyprep-M column, toluene, room temperature, 16 mL/min flow rate). (b) UV−vis absorption spectrum of the toluene solution of N@C_{60}-1-CuPc (solid line), which is similar to the superposition of the spectra of the phthalocyanine aldehyde (dashed line) and the functionalized fullerene reference (dotted line). (c) High-resolution MALDI-TOF mass spectrum of N@C_{60}-1-CuPc in a dithranol matrix in positive mode with the theoretical predictions. The dominant peaks are from the empty cage dyad (blue lines), but the weak MS peaks representing the endohedral fullerene dyad (red lines) are also detectable.

product peak relative to the whole HPLC curve), the unreacted reagents were collected and reused for a second reaction batch to improve the overall conversion ratio to higher than 40%. Apart from the dyads, a pyrrolidine-functionalized fullerene, F-C_{60} (structure shown in Supporting Information S1) was also prepared according to the literature[32] and was applied as the UV−vis reference.

The successful formation of the products was manifested by UV−vis absorption spectroscopy and mass spectrometry (MS). As depicted in Figure 2b, the UV−vis spectrum of the toluene solution of N@C_{60}-1-CuPc (solid line) is a superposition of the absorption features of the phthalocyanine aldehyde (dashed line) and the functionalized fullerene reference (dotted line), which suggests the existence of both the phthalocyanine and fullerene moieties in the product molecule. In addition, the characteristic absorption band at 430 nm indicating the 1,2-adduct structure of the fullerene[28,33] can also be observed in the spectrum. The MS characterization of N@C_{60}-1-CuPc is shown in Figure 2c, where the experimental peaks (black) are consistent with the combination of the theoretical predictions for C_{60}-1-CuPc (blue) and N@C_{60}-1-CuPc (red). As a result of the 1% concentration of the endohedral fullerene and the potential fragmentation during the ionization, the dominant peaks are due to the empty cage dyad, but the weak MS peaks representing the endohedral fullerene dyad remain detectable and agree nicely with the theoretical predictions. UV−vis and MS characterization data were also obtained for N@C_{60}-2-CuPc and N@C_{60}-1-ZnPc (Supporting Information S2).

Analysis of the Electron Spin Properties. We applied continuous-wave electron paramagnetic resonance (CW-EPR) spectroscopy to study the spin properties of the synthesized dyads. Among the three dyads, N@C_{60}-1-CuPc and N@C_{60}-2-CuPc are multispin systems while N@C_{60}-1-ZnPc contains just one electron spin center. N@C_{60} and CuPc, which contain the $^4S_{3/2}$ state of the endohedral nitrogen atom and the $3d^9$ electron configuration of the central Cu^{2+} ion, respectively, are spin-active, whereas ZnPc is spin-silent. Compared with N@C_{60}-1-ZnPc, the spin signals from the multispin dyads are more complicated. Fortunately, as shown by the full-range spectrum of N@C_{60}-1-CuPc in Figure 3a, the signals from the copper spin and the endohedral nitrogen spin do not overlap, enabling us to interpret them separately. Herein we mainly focused on the electron spin of the N@C_{60} moiety rather than that of CuPc because of the better sensitivity of its sharp signal and its higher relevance to the spin−spin interaction. Limited by the purity of the N@C_{60}/C_{60} mixture, in the Cu dyad samples only 1% of the dyads contained the N@C_{60} spin but 100% contained the CuPc spin. Hence, 99% of the CuPc spins were just covalently linked with empty cages, whereas every N@C_{60} spin was coupled with a CuPc spin.

The zoomed-in solution CW-EPR spectra of the nitrogen spin region (Figure 3b) were studied first. For pristine N@C_{60}, N@C_{60}-1-ZnPc, N@C_{60}-1-CuPc, and N@C_{60}-2-CuPc dissolved in toluene (10^{-5} M), we obtained the same triplet pattern, which is attributed to the hyperfine coupling (HFC) between the nitrogen electron spin ($S = {}^3/_2$) and the nitrogen nuclear spin ($I = 1$). The absence of any extra spectral splitting in the dyad spectra leads to two conclusions: (1) the molecules tumble rapidly in their respective toluene solutions, and therefore, all of the anisotropic spin features having a traceless tensor, such as the potential zero-field splitting (ZFS) peaks and electron spin dipolar coupling features, are averaged out to zero; (2) there is no discernible electron spin−spin exchange

DOI: 10.1021/jacs.5b11641
J. Am. Chem. Soc. 2016, 138, 1313−1319

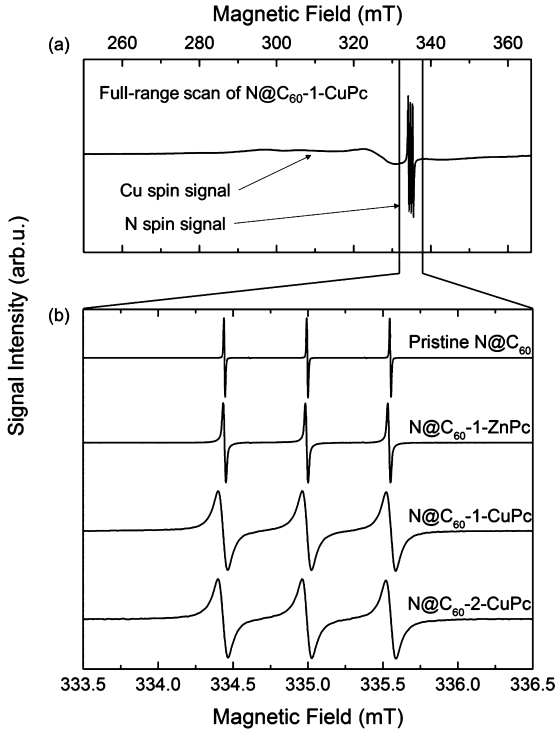

Figure 3. (a) Solution CW-EPR spectra of N@C_{60}-1-CuPc (full range) highlighting the fact that the spin signals of Cu and N do not overlap. (b) Comparison of the solution CW-EPR spectra of pristine N@C_{60}, N@C_{60}-1-ZnPc, N@C_{60}-1-CuPc, and N@C_{60}-2-CuPc, which focuses on the nitrogen spin region (all of the measurements were taken with 10^{-5} M toluene solution samples at room temperature).

coupling in either of the multispin dyads because of the near-perfect protection of the fullerene cage, which excludes the probability of any spin density overlap.[21] Such an exotic phenomenon is different from other diradical molecular systems[34−36] having similar spin separations but showing exchange coupling splitting in their solution spectra.

In contrast to the similarity of the spectral splitting pattern, the line width, which is inversely proportional to the relaxation time, varies, providing us with a qualitative approach to compare the electron spin relaxation times for the compounds. The averaged peak-to-peak line width (ΔH_{pp}) for pristine N@C_{60} was measured to be less than 3 μT, representing an ultralong relaxation time, consistent with previous reports.[8] The averaged ΔH_{pp} of N@C_{60}-1-ZnPc is slightly broadened as a result of the degradation of the high molecular symmetry,[37] the relatively lower tumbling rate,[38] and the proton nuclear influence,[39] but it is still as sharp as 18 μT. For the multispin molecules, N@C_{60}-1-CuPc and N@C_{60}-2-CuPc, the signals become substantially broader, with the averaged ΔH_{pp} increasing to 60 and 63 μT, respectively. Since physically mixing N@C_{60} with CuPc does not show such a significant broadening effect, even at very high concentrations (Supporting Information S3), this phenomenon is attributed to the chemical linkage of the two spin centers, which decreases the relaxation time of the endohedral spin considerably because of the strong intramolecular electron spin interaction. Since electron spin exchange coupling was ruled out by the splitting pattern analysis, the electron spin dipolar coupling has to be the major intermolecular spin interaction mechanism.

Having established the existence of dipolar coupling, we went on to measure the solid-state CW-EPR spectra, which allowed us to extract more information on the electron spin dipolar coupling strength by immersing the sample tube in liquid nitrogen and stabilizing the measurement conditions at 100 K with a nitrogen-flow cryostat. Benefiting from the well-controlled reaction conditions, all of the solid-state spectra of pristine N@C_{60}, N@C_{60}-1-ZnPc, N@C_{60}-1-CuPc, and N@C_{60}-2-CuPc have excellent signal-to-noise ratios and are free of the commonly reported $S = {}^1/_2$ impurity in the functionalized N@C_{60} powder spectra.[40,41] The nitrogen spin regions of these spectra are shown in Figure 4.

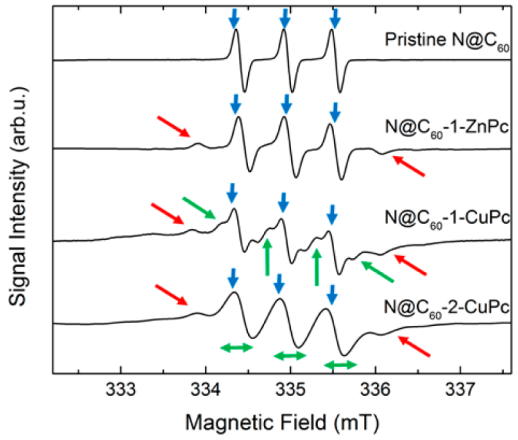

Figure 4. Solid-state CW-EPR spectra (nitrogen spin region) of pristine N@C_{60}, N@C_{60}-1-ZnPc, N@C_{60}-1-CuPc, and N@C_{60}-2-CuPc. All of the measurements were taken with frozen 10^{-5} M toluene solutions at 100 K. The peaks of hyperfine coupling (HFC) and zero-field splitting (ZFS) are labeled with blue and red arrows, respectively. The dipolar coupling features, such as fine shoulder peaks and line broadening, are marked with green arrows.

The solid-state CW-EPR spectrum of pristine N@C_{60} shows only three HFC peaks, which commonly exist in all of the spectra (indicated by blue arrows). The absence of any extra splitting results from the I_h symmetry of the fullerene cage and the effective dilution of the toluene matrix in amorphous form. In comparison, N@C_{60}-1-ZnPc, which has a lower molecular symmetry, shows characteristic weak and broad ZFS side peaks (marked by red arrows). According to the spectrum simulation (Supporting Information S4), the axial ZFS parameter D was determined to be 14.2 MHz, which is typical for N@C_{60} pyrrolidine derivatives. The evenly sized HFC peaks as well as the simulated isotropic HFC constant (A_{iso} = 15.4 MHz) confirm that the HFC remains isotropic, providing further experimental evidence concerning the influence of functionalization of pyrrolidine addends on HFC. There are contradictory reports about this in the literature.[38,41]

The spectra of N@C_{60}-1-CuPc and N@C_{60}-2-CuPc in the nitrogen spin region appear different from that for N@C_{60}-1-ZnPc (see the fine features marked by green arrows), even though these three molecules should have very similar ZFS and HFC features because of the nearly identical structures and electron configurations in the fullerene moiety. We ascribe both of the additional fine features to the variant effects of electron spin dipolar coupling, which was shown to be the major intramolecular spin interaction by the above solution CW-EPR study. However, the fine features of the dipolar coupling in the two spectra still vary. The spectrum of N@C_{60}-1-CuPc has more obvious splitting with shoulder peaks emerging next to the HFC peaks, whereas the spectrum of N@C_{60}-2-CuPc

DOI: 10.1021/jacs.5b11641
J. Am. Chem. Soc. 2016, 138, 1313−1319

shows broadened HFC peaks only. We explain such splitting variation as follows: The extent of the splitting is proportional to the coupling strength,[42] and the dipolar coupling strength is reciprocally proportional to the cube of the spin−spin distance r (giving the factor of $1/r^3$ in the model in Figure 5a).

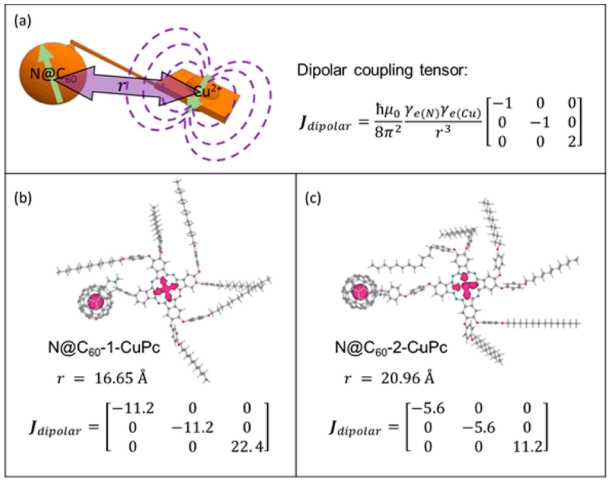

Figure 5. (a) Illustration and equation of the dependence of the electron spin dipolar coupling on the spin separation. (b, c) Spin density distributions of the multispin dyads in their corresponding preferential configurations (contour levels are 1×10^{-3} e/au), on the basis of which the electron spin distances and dipolar coupling strengths were calculated.

According to the calculated spin density distributions and preferential configurations for the multispin dyads (Figure 5b,c), we theoretically estimated that the separations between the spin centers are 16.65 Å in N@C_{60}-1-CuPc and 20.96 Å in N@C_{60}-2-CuPc. Subsequently, we further determined that the coupling strength for N@C_{60}-1-CuPc (11.2 MHz) is twice that for N@C_{60}-2-CuPc (5.6 MHz), which qualitatively explains the splitting variation in their spectra. To the best of our knowledge, this is the first comparison between the solid-state spectra of two variably distanced endohedral fullerene multispin systems. In addition, we have demonstrated experimentally the chemical tunability of the dipolar coupling strength between the potential spin qubits N@C_{60} and CuPc by changing the length of the bridging unit between them.

Explanation of the Low Coupling Strength. Despite the successful qualitative interpretation of the dipolar splitting, a quantitative one remains far more challenging. With a comprehensive spin Hamiltonian model covering the tensor value and direction, the initial simulation details are described in Supporting Information S5. The experimental spectra have less prominent dipolar coupling features than the simulated ones. We estimate that the apparent dipolar coupling strengths in the experimental data are ca. 30% weaker than the theoretical predictions of 11.2 and 5.6 MHz for the two multispin dyads. The reason for such deviations is discussed below.

The first reason one may argue is the presence of thermal vibrations for the preferential conformation. Since all of the distances we used for the fittings were based on density functional theory calculations, which are optimized at 0 K whereas the experimental data were measured at 100 K, thermal vibrations might lead to larger spin separations in both dyads, which would consequently lower the resulting coupling strength. However, according the dynamic MM2 simulation, the dyad molecules vibrate insignificantly because of the relatively rigid molecular structure. We have shown that the simulation model is insensitive to any potential error existing in the relative angle caused by the sp^3 bond rotation (Supporting Information S8A). Moreover, the unchanged CW-EPR spectra for both dyads as the measurement temperature was decreased to 77 K also suggest that the temperature does not play a crucial role in the spectral deviations. Hence, the fitting failure cannot be due to the thermal vibrations of the preferential conformation.

Another potential explanation could be the magnetic shielding effect of the fullerene cage, as the ring-current effect of the π-conjugated electrons of the fullerene cage is capable of partial shielding of the dipolar magnetic field experienced by the endohedral spin. However, on the basis of the shielding effect reported previously (6 ppm for ^{3}He@C_{60} vs free ^{3}He[43] and 19 ppm for N@C_{70} vs N@C_{60}[44]), the shielding effect of the fullerene cage should be completely negligible compared with such a significant weakening effect.

With the above reasons excluded, we conclude that aggregation of the phthalocyanine moieties in the form of stacking can indirectly decrease the apparent dipolar coupling strength. It has been reported that CuPc tends to aggregate[45,46] and that the aggregation in the α phase can lead to the formation of an antiferromagnetic array.[25,47,48] For the specific CuPc system and experimental conditions discussed in this work, we demonstrated the existence of an aggregation effect and its resulting antiferromagnetism by dynamic light scattering (DLS) (Supporting Information S6) and EPR analysis of the copper spin (Supporting Information S7), respectively. Figure 6 compares the dyad molecules in the nonaggregated and aggregated cases. In the nonaggregated case, the standard dipolar coupling takes place and the calculated dipolar coupling strength is feasible. When the CuPc moieties aggregate, the dipolar field of the copper spin experienced by the nitrogen spin is significantly suppressed because the antiparallel alignment of the copper spins can neutralize the field. Therefore, a weaker apparent dipolar coupling strength can be expected.

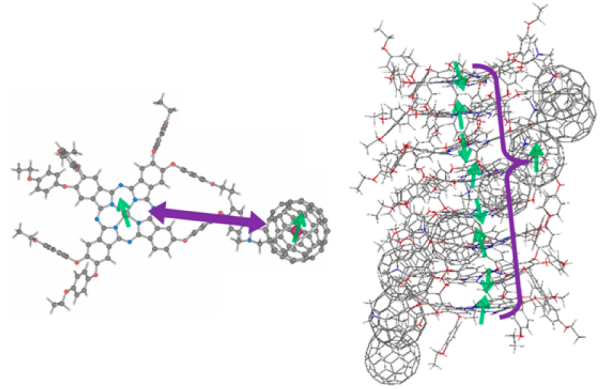

Figure 6. Schematic diagram illustrating the different dipolar coupling strengths experienced by the nitrogen spin in the nonaggregated and aggregated cases. (Only one nitrogen spin is expected in the aggregated cluster because of the 1% endohedral fullerene content in the reagent.)

In order to amend the direct simulation model, which is limited to an intramolecular layer, and to quantitatively interpret the low coupling strength, the aggregation and

DOI: 10.1021/jacs.5b11641
J. Am. Chem. Soc. 2016, 138, 1313−1319

antiferromagnetism have to be taken into consideration. However, the weakening effect depends on the size of the aggregate, and it is difficult to individually analyze the varying extent of aggregation in the sample. By observing that the dipolar coupling strength converges to zero as the size of the aggregated cluster grows, we treated the coupling strength as zero in all of the aggregated cases by a complete suppression approximation. The dipolar field after the neutralization of the antiferromagnetism is negligible compared with that in the nonaggregated case, so the assumption holds in the majority of cases of the aggregated clusters (see Supporting Information S8B). The only considerable coupling strength is in clusters formed by aggregation of a small number of molecules, but it will merely lead to an insignificant overestimation of the ratio of the nonaggregated case to the aggregated case and impose no effect on the spectral simulations. Therefore, we combined the spin Hamiltonian model in Supporting Information S5 with the complete suppression approximation and did the simulations by using the aggregation percentage as a fitting parameter. Figure 7 shows that the case of 75% nonaggregated plus 25% aggregated was used to fit the spectrum of N@C_{60}-1-CuPc, while the case of 73% nonaggregated plus 27% aggregated was used to fit the spectrum of N@C_{60}-2-CuPc.

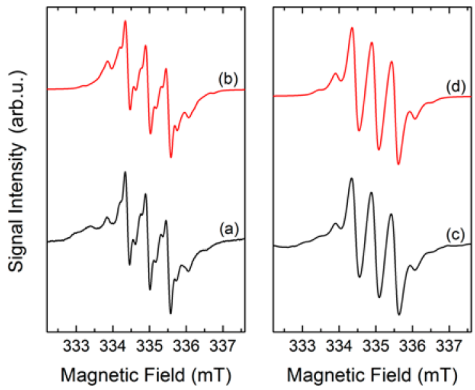

Figure 7. (a, c) Solid-state CW-EPR spectra of (a) N@C_{60}-1-CuPc and (c) N@C_{60}-2-CuPc and (b, d) the corresponding simulation results.

Concentration-Dependent Dipolar Coupling Strength. In order to confirm the influence of aggregation on the apparent dipolar coupling strength and to justify the complete suppression approximation, we measured additional CW-EPR spectra of N@C_{60}-1-CuPc at different concentrations and fitted the individual data. All of the concentration-dependent spectra (Figure 8a) were taken with a low microwave power of 3.170 μW, which maintained the linearity of the signal intensity. Therefore, the observed spectral variation did not originate from power saturation but had to be caused by the variation of the aggregation effect in progressively more concentrated samples. Since the dipolar coupling features became more significant when the sample got diluted and less aggregated, we confirmed the suppression effect of the aggregation and its resulting antiferromagnetism on the apparent dipolar coupling strength. The increasing trend of the simulated aggregation percentage (Figure 8b) is consistent with the dynamic light scattering data (Supporting Information S6) and previously reported results.[49] Hence, the complete suppression approximation is validated.

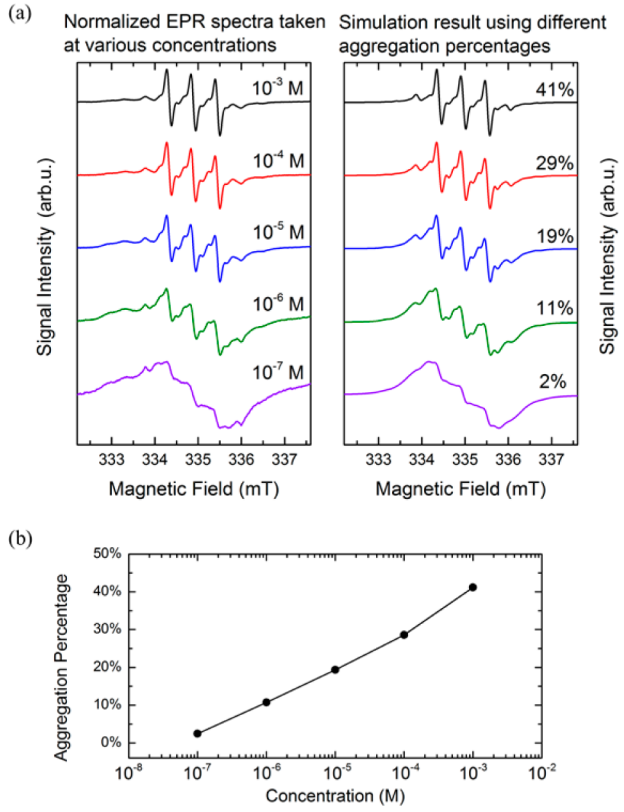

Figure 8. (a) Solid-state CW-EPR spectra of frozen toluene solutions (100 K) of N@C_{60}-1-CuPc taken at various concentrations and the corresponding simulation results with different aggregation percentages. (b) Concentration dependence of the aggregation percentage in N@C_{60}-1-CuPc frozen toluene solution samples based on the simulation results.

The solution concentration dependence opens a new way of tuning the dipolar coupling strength in this dyad system. We can reversibly turn on the dipolar coupling by diluting the sample and turn off the dipolar coupling by concentrating the sample (Supporting Information S9). Compared with tuning the dipolar coupling chemically by adjusting the size of the space group, changing the concentration does not require any change the molecular structure. Since the aggregation effect changes gradually with the concentration, the sample concentration cannot enable us to turn the dipolar coupling on and off in a real device. However, if one could adjust the dyad molecules to make the aggregation effect strongly depend on any external stimulus, such as pH, temperature, or electric potential, then control of the dipolar coupling could be realized at the device level. Our initial DLS experiment showed that one can change the aggregation properties of the dyad by altering the pH (Supporting Information S10), but in order to show the spin signal and dipolar coupling features, further confirmation of the compatibility of the acidic conditions and the endohedral fullerene is required. This is a first step in this direction.

CONCLUSIONS

We have synthesized three different endohedral fullerene–phthalocyanine dyads. Two of them were multispin systems containing variable spin distances for studying the dipolar coupling, and the third one, a dyad with a diamagnetic Zn ion, was used as the reference. All of the products were characterized by UV–vis spectroscopy, high-resolution

DOI: 10.1021/jacs.5b11641
J. Am. Chem. Soc. 2016, 138, 1313–1319

MALDI-TOF mass spectrometry, and solution and solid-state CW-EPR spectroscopy. From the solution and solid-state CW-EPR analysis, we determined the spectral features of the dipolar coupling and compared the spectral differences in the two dyads having variant spin−spin distance, demonstrating that the chemical adjustment of the spacer group is enough to change the dipolar coupling strength. With the additional discussion of the aggregation and antiferromagnetism of the CuPc moiety, we managed to quantitatively interpret the experimental results with a simulation model and discovered a new way of tuning the dipolar coupling strength that utilizes the formation and deformation of the antiferromagnetic array of CuPc to turn the dipolar coupling off and on, respectively.

EXPERIMENTAL SECTION

Preparation of the Spin-Enriched N@C_{60}/C_{60} Mixture. As a precursor for the endohedral fullerene moieties in the dyads, a mixture of N@C_{60} in C_{60} was obtained via an optimized ion implantation procedure.[50] Its purity was then enhanced from 100 ppm to 1% by recycled HPLC[51−53] using 15-PBB and 5-PBB columns (Nacalai Tesque, Kyoto, Japan). All of the spin percentages were determined by C_{60}-calibrated UV−vis spectroscopy and 2,2,6,6-tetramethylpiperidine 1-oxyl (TEMPO)-calibrated CW-EPR spectroscopy.

Synthesis of Phthalocyanine Aldehydes. As precursors for the phthalocyanine moieties in the dyads, the aldehydes CuPc-1-CHO, CuPc-2-CHO, and ZnPc-1-CHO were synthesized through a one-pot reaction with 4,5-bis(4-dodecyloxyphenoxy)phthalonitrile, the corresponding central metal ions, and 4-(4-formylphenoxy)phthalonitrile (or 4-(4-(4-formylphenoxy)phenoxy)phthalonitrile for the long-distance dyad). The reaction schemes and characterization data for them are listed in Supporting Information S11.

MALDI-TOF MS. MALDI-TOF measurements were performed on a Bruker Microflex LT spectrometer in positive reflective mode with dithranol and CsI_3 as the matrix and calibration reference, respectively.

CW-EPR Spectroscopy. X-band CW-EPR measurements were performed on Magnettech Miniscope MS200 and Bruker EMX spectrometers. Simulations of CW-EPR spectra were performed using the EASYSPIN software package.[54]

Quantum-Chemical Calculations. The geometry optimization and spin distribution calculations were performed at the PM3 level followed by the B3LYP/6-311G(d) level using the Gaussian 03 program[55] on an HPC2500 computer. The frequency analyses were performed at the same level.

ASSOCIATED CONTENT

Supporting Information

The Supporting Information is available free of charge on the ACS Publications website at DOI: 10.1021/jacs.5b11641.

Molecular structure of F-C_{60}, parallel UV/vis and MS characterizations of N@C_{60}-2-CuPc and N@C_{60}-1-ZnPc, line width comparison of solution EPR spectra, simulation of the spectrum of the frozen N@C_{60}-1-ZnPc toluene solution, simulations of the spectra of the multispin dyads before aggregation was considered, experimental evidence for aggregation and antiferromagnetism, and synthesis and characterization for the phthalocyanine aldehyde precursors (PDF)

AUTHOR INFORMATION

Corresponding Authors

*imahori@scl.kyoto-u.ac.jp

*kyriakos.porfyrakis@materials.ox.ac.uk

Author Contributions

‖S.Z. and M.Y. contributed equally.

Notes

The authors declare no competing financial interest.

ACKNOWLEDGMENTS

This work was supported by the EPSRC (EP/K030108/1) and by a Grant-in-Aid (25620148 to H.I.) and the WPI Initiative of MEXT, Japan. We thank Yuta Takano, Panagiotis Dallas, Yo Shimizu, and Gregory Rogers for helpful discussions and Christina Foldbjerg for technical support. We acknowledge CAESR and Dr. William Myers for the instrument support during the EPR measurements. S.Z. thanks the National University of Defense Technology and Prof. Haifeng Cheng for the studentship and support. M.Y. is grateful for a JSPS Fellowship for Young Scientists.

REFERENCES

(1) Yamada, M.; Kurihara, H.; Suzuki, M.; Saito, M.; Slanina, Z.; Uhlik, F.; Aizawa, T.; Kato, T.; Olmstead, M. M.; Balch, A. L.; Maeda, Y.; Nagase, S.; Lu, X.; Akasaka, T. *J. Am. Chem. Soc.* **2015**, *137*, 232.

(2) Yamada, M.; Kurihara, H.; Suzuki, M.; Guo, J. D.; Waelchli, M.; Olmstead, M. M.; Balch, A. L.; Nagase, S.; Maeda, Y.; Hasegawa, T.; Lu, X.; Akasaka, T. *J. Am. Chem. Soc.* **2014**, *136*, 7611.

(3) Popov, A. A.; Pykhova, A. D.; Ioffe, I. N.; Li, F.-F.; Echegoyen, L. *J. Am. Chem. Soc.* **2014**, *136*, 13436.

(4) Morinaka, Y.; Sato, S.; Wakamiya, A.; Nikawa, H.; Mizorogi, N.; Tanabe, F.; Murata, M.; Komatsu, K.; Furukawa, K.; Kato, T.; Nagase, S.; Akasaka, T.; Murata, Y. *Nat. Commun.* **2013**, *4*, 1554.

(5) Popov, A. A.; Yang, S.; Dunsch, L. *Chem. Rev.* **2013**, *113*, 5989.

(6) Lu, X.; Feng, L.; Akasaka, T.; Nagase, S. *Chem. Soc. Rev.* **2012**, *41*, 7723.

(7) Wang, T.; Wu, J.; Xu, W.; Xiang, J.; Lu, X.; Li, B.; Jiang, L.; Shu, C.; Wang, C. *Angew. Chem., Int. Ed.* **2010**, *49*, 1786.

(8) Morton, J. J. L.; Tyryshkin, A. M.; Ardavan, A.; Porfyrakis, K.; Lyon, S. A.; Briggs, G. A. D. *J. Chem. Phys.* **2006**, *124*, 014508.

(9) Brown, R. M.; Ito, Y.; Warner, J. H.; Ardavan, A.; Shinohara, H.; Briggs, G. A. D.; Morton, J. J. L. *Phys. Rev. B: Condens. Matter Mater. Phys.* **2010**, *82*, 033410.

(10) Harneit, W. *Phys. Rev. A: At., Mol., Opt. Phys.* **2002**, *65*, 032322.

(11) Benjamin, S. C.; Ardavan, A.; Briggs, G. A. D.; Britz, D. A.; Gunlycke, D.; Jefferson, J.; Jones, M. A. G.; Leigh, D. F.; Lovett, B. W.; Khlobystov, A. N.; Lyon, S. A.; Morton, J. J. L.; Porfyrakis, K.; Sambrook, M. R.; Tyryshkin, A. M. *J. Phys.: Condens. Matter* **2006**, *18*, S867.

(12) Wesenberg, J.; Ardavan, A.; Briggs, G.; Morton, J.; Schoelkopf, R.; Schuster, D.; Mølmer, K. *Phys. Rev. Lett.* **2009**, *103*, 070502.

(13) Yang, W. L.; Xu, Z. Y.; Wei, H.; Feng, M.; Suter, D. *Phys. Rev. A: At., Mol., Opt. Phys.* **2010**, *81*, 032303.

(14) Plant, S. R.; Jevric, M.; Morton, J. J. L.; Ardavan, A.; Khlobystov, A. N.; Briggs, G. A. D.; Porfyrakis, K. *Chem. Sci.* **2013**, *4*, 2971.

(15) Feng, M.; Twamley, J. *Phys. Rev. A: At., Mol., Opt. Phys.* **2004**, *70*, 032318.

(16) Morton, J. J. L.; Tyryshkin, A. M.; Ardavan, A.; Porfyrakis, K.; Lyon, S. a.; Briggs, G. A. D. *Phys. Rev. Lett.* **2005**, *95*, 200501.

(17) Ju, C.; Suter, D.; Du, J. *Phys. Lett. A* **2011**, *375*, 1441.

(18) Morton, J. J. L.; Tyryshkin, A. M.; Ardavan, A.; Benjamin, S. C.; Porfyrakis, K.; Lyon, S. A.; Briggs, G. A. D. *Nat. Phys.* **2006**, *2*, 40.

(19) Filidou, V.; Simmons, S.; Karlen, S. D.; Giustino, F.; Anderson, H. L.; Morton, J. J. L. *Nat. Phys.* **2012**, *8*, 596.

(20) Ju, C.; Suter, D.; Du, J. *Phys. Rev. A: At., Mol., Opt. Phys.* **2007**, *75*, 012318.

(21) Liu, G.; Khlobystov, A. N.; Charalambidis, G.; Coutsolelos, A. G.; Briggs, G. A. D.; Porfyrakis, K. *J. Am. Chem. Soc.* **2012**, *134*, 1938.

(22) Wu, B.; Wang, T.; Feng, Y.; Zhang, Z.; Jiang, L.; Wang, C. *Nat. Commun.* **2015**, *6*, 6468.

(23) Farrington, B. J.; Jevric, M.; Rance, G. A.; Ardavan, A.; Khlobystov, A. N.; Briggs, G. A. D.; Porfyrakis, K. *Angew. Chem., Int. Ed.* **2012**, *51*, 3587.

DOI: 10.1021/jacs.5b11641
J. Am. Chem. Soc. 2016, 138, 1313−1319

(24) Warner, M.; Din, S.; Tupitsyn, I. S.; Morley, G. W.; Stoneham, a M.; Gardener, J. a; Wu, Z.; Fisher, A. J.; Heutz, S.; Kay, C. W. M.; Aeppli, G. *Nature* **2013**, *503*, 504.
(25) Wang, H.; Mauthoor, S.; Din, S.; Gardener, J. a.; Chang, R.; Warner, M.; Aeppli, G.; McComb, D. W.; Ryan, M. P.; Wu, W.; Fisher, A. J.; Stoneham, M.; Heutz, S. *ACS Nano* **2010**, *4*, 3921.
(26) Hayashi, H.; Nihashi, W.; Umeyama, T.; Matano, Y.; Seki, S.; Shimizu, Y.; Imahori, H. *J. Am. Chem. Soc.* **2011**, *133*, 10736.
(27) Maggini, M.; Scorrano, G.; Prato, M. *J. Am. Chem. Soc.* **1993**, *115*, 9798.
(28) Prato, M.; Maggini, M. *Acc. Chem. Res.* **1998**, *31*, 519.
(29) Waiblinger, M.; Lips, K.; Harneit, W.; Weidinger, A.; Dietel, E.; Hirsch, A. *Phys. Rev. B: Condens. Matter Mater. Phys.* **2001**, *64*, 159901.
(30) Liu, G.; Khlobystov, A. N.; Ardavan, A.; Briggs, G. A. D.; Porfyrakis, K. *Chem. Phys. Lett.* **2011**, *508*, 187.
(31) Zhou, S.; Rašović, I.; Briggs, G. A. D.; Porfyrakis, K. *Chem. Commun.* **2015**, *51*, 7096.
(32) Imahori, H.; Ozawa, S.; Ushida, K.; Takahashi, M.; Azuma, T.; Ajavakom, A.; Akiyama, T.; Hasegawa, M.; Taniguchi, S.; Okada, T.; Sakata, Y. *Bull. Chem. Soc. Jpn.* **1999**, *72*, 485.
(33) Bensasson, R. V.; Bienvenüe, E.; Fabre, C.; Janot, J. M.; Land, E. J.; Leach, S.; Leboulaire, V.; Rassat, A.; Roux, S.; Seta, P. *Chem. - Eur. J.* **1998**, *4*, 270.
(34) Shultz, D. A.; Mussari, C. P.; Ramanathan, K. K.; Kampf, J. W. *Inorg. Chem.* **2006**, *45*, 5752.
(35) Shultz, D. A.; Fico, R. M.; Bodnar, S. H.; Kumar, R. K.; Vostrikova, K. E.; Kampf, J. W.; Boyle, P. D. *J. Am. Chem. Soc.* **2003**, *125*, 11761.
(36) Ayabe, K.; Sato, K.; Nishida, S.; Ise, T.; Nakazawa, S.; Sugisaki, K.; Morita, Y.; Toyota, K.; Shiomi, D.; Kitagawa, M.; Takui, T. *Phys. Chem. Chem. Phys.* **2012**, *14*, 9137.
(37) Knapp, C.; Dinse, K. P.; Pietzak, B.; Waiblinger, M.; Weidinger, A. *Chem. Phys. Lett.* **1997**, *272*, 433.
(38) Zhang, J.; Morton, J. J. L.; Sambrook, M. R.; Porfyrakis, K.; Ardavan, A.; Briggs, G. A. D. *Chem. Phys. Lett.* **2006**, *432*, 523.
(39) Morton, J. J. L.; Tyryshkin, A. M.; Ardavan, A.; Porfyrakis, K.; Lyon, S. a.; Briggs, G. A. D. *Phys. Rev. B: Condens. Matter Mater. Phys.* **2007**, *76*, 085418.
(40) Goedde, B.; Waiblinger, M.; Jakes, P.; Weiden, N.; Dinse, K. P.; Weidinger, A. *Chem. Phys. Lett.* **2001**, *334*, 12.
(41) Franco, L.; Ceola, S.; Corvaja, C.; Bolzonella, S.; Harneit, W.; Maggini, M. *Chem. Phys. Lett.* **2006**, *422*, 100.
(42) Banham, J. E.; Baker, C. M.; Ceola, S.; Day, I. J.; Grant, G. H.; Groenen, E. J. J.; Rodgers, C. T.; Jeschke, G.; Timmel, C. R. *J. Magn. Reson.* **2008**, *191*, 202.
(43) Saunders, M.; Jiménez-Vázquez, H. A.; Cross, R. J.; Mroczkowski, S.; Freedberg, D. I.; Anet, F. A. L. *Nature* **1994**, *367*, 256.
(44) Lips, K.; Waiblinger, M.; Pietzak, B.; Weidinger, A. *Phys. Status Solidi A* **2000**, *177*, 81.
(45) Monahan, A. R.; Brado, J. A.; DeLuca, A. F. *J. Phys. Chem.* **1972**, *76*, 446.
(46) Monahan, A. R.; Brado, J. A.; DeLuca, A. F. *J. Phys. Chem.* **1972**, *76*, 1994.
(47) Serri, M.; Wu, W.; Fleet, L. R.; Harrison, N. M.; Hirjibehedin, C. F.; Kay, C. W. M.; Fisher, A. J.; Aeppli, G.; Heutz, S. *Nat. Commun.* **2014**, *5*, 3079.
(48) Heutz, S.; Mitra, C.; Wu, W.; Fisher, A. J.; Kerridge, A.; Stoneham, M.; Harker, T. H.; Gardener, J.; Tseng, H. H.; Jones, T. S.; Renner, C.; Aeppli, G. *Adv. Mater.* **2007**, *19*, 3618.
(49) Camp, P. J.; Jones, A. C.; Neely, R. K.; Speirs, N. M. *J. Phys. Chem. A* **2002**, *106*, 10725.
(50) Almeida Murphy, T.; Pawlik, T.; Weidinger, A.; Höhne, M.; Alcala, R.; Spaeth, J. M. *Phys. Rev. Lett.* **1996**, *77*, 1075.
(51) Kanai, M.; Porfyrakis, K.; Briggs, G. A. D.; Dennis, T. J. S. *Chem. Commun.* **2004**, *40*, 210.
(52) Jakes, P.; Dinse, K. P.; Meyer, C.; Harneit, W.; Weidinger, A. *Phys. Chem. Chem. Phys.* **2003**, *5*, 4080.
(53) Plant, S. R.; Porfyrakis, K. *Analyst* **2014**, *139*, 4519.
(54) Stoll, S.; Schweiger, A. *J. Magn. Reson.* **2006**, *178*, 42.
(55) Frisch, M. J.; Trucks, G. W.; Schlegel, H. B.; Scuseria, G. E.; Robb, M. A.; Cheeseman, J. R.; Montgomery, J. A., Jr.; Vreven, T.; Kudin, K. N.; Burant, J. C.; Millam, J. M.; Iyengar, S. S.; Tomasi, J.; Barone, V.; Mennucci, B.; Cossi, M.; Scalmani, G.; Rega, N.; Petersson, G. A.; Nakatsuji, H.; Hada, M.; Ehara, M.; Toyota, K.; Fukuda, R.; Hasegawa, J.; Ishida, M.; Nakajima, T.; Honda, Y.; Kitao, O.; Nakai, H.; Klene, M.; Li, X.; Knox, J. E.; Hratchian, H. P.; Cross, J. B.; Bakken, V.; Adamo, C.; Jaramillo, J.; Gomperts, R.; Stratmann, R. E.; Yazyev, O.; Austin, A. J.; Cammi, R.; Pomelli, C.; Ochterski, J. W.; Ayala, P. Y.; Morokuma, K.; Voth, G. A.; Salvador, P.; Dannenberg, J. J.; Zakrzewski, V. G.; Dapprich, S.; Daniels, A. D.; Strain, M. C.; Farkas, O.; Malick, D. K.; Rabuck, A. D.; Raghavachari, K.; Foresman, J. B.; Ortiz, J. V.; Cui, Q.; Baboul, A. G.; Clifford, S.; Cioslowski, J.; Stefanov, B. B.; Liu, G.; Liashenko, A.; Piskorz, P.; Komaromi, I.; Martin, R. L.; Fox, D. J.; Keith, T.; Al-Laham, M. A.; Peng, C. Y.; Nanayakkara, A.; Challacombe, M.; Gill, P. M. W.; Johnson, B.; Chen, W.; Wong, M. W.; Gonzalez, C.; Pople, J. A. *Gaussian 03*; Gaussian, Inc.: Wallingford, CT, 2004.

DOI: 10.1021/jacs.5b11641
J. Am. Chem. Soc. 2016, 138, 1313−1319